



\mathcal{C}^1 -curved finite elements and applications to plate and shell problems

M. Bernadou

*Institut National de Recherche en Informatique et en Automatique, Domaine de Voluceau, B.P. 105, Rocquencourt,
78153 Le Chesnay Cédex, France*

Received 19 June 1992

Abstract

Many thin-plate and thin-shell problems are set on plane reference domains with a curved boundary. Their approximation by conforming finite-element methods requires \mathcal{C}^1 -curved finite elements entirely compatible with the associated \mathcal{C}^1 -rectilinear finite elements. In this contribution we introduce a \mathcal{C}^1 -curved finite element compatible with the P_5 -Argyris element, we study its approximation properties, and then, we use such an element to approximate the solution of thin-plate or thin-shell problems set on a plane-curved boundary domain. We prove the convergence and we get a priori asymptotic error estimates which show the very high degree of accuracy of the method. Moreover we obtain criteria to observe when choosing the numerical integration schemes in order to preserve the order of the error estimates obtained for exact integration.

Key words: \mathcal{C}^1 -curved finite elements; Plate and shell problems

1. Introduction

The use of the P_5 -Argyris finite element [1] for the approximation of thin-plate and thin-shell problems formulated on plane-polygonal domains Ω leads to numerical methods with a very high degree of accuracy: the error estimate in the energy norm is $O(h^4)$, where $h = \sup_{K \in \mathcal{T}_h} \text{diam}(K)$ where \mathcal{T}_h denotes the triangulation of Ω [2,5]. The aim of this contribution is to extend such properties to the case of thin-plate or thin-shell problems formulated on plane *curved* boundary domains. That means, we will have three different approximations to combine:

- (i) the approximation of the displacement;
- (ii) the approximation which arises from the use of a numerical integration scheme;
- (iii) the approximation of the boundary $\partial\Omega$.

Of course, the basic idea is to obtain criteria which give the same asymptotic error estimates for the three approximations, i.e., $O(h^4)$ in the energy norm.

The results that we briefly describe hereafter are detailed in [3,4] regarding mathematical aspects and in [6,7] regarding the implementation and some numerical experiments.

Concerning the definition of curved finite elements and their numerical analysis, it is worth mentioning [14,29–31] for second-order problems and [12–14,20,21,24–28] for fourth-order problems. Let us also mention [10,16,18] where \mathcal{E}^1 -curved finite elements are considered for which the finite-dimensional space is polynomial upon the curved current triangle T ; but the analysis of the approximation due to the numerical integration seems to be out of reach with such a method.

2. Construction and interpolation properties of a \mathcal{E}^1 -curved finite element

Let Ω be a plane domain of \mathbb{R}^2 with an orthonormal basis $(0, e_1, e_2)$. We assume that the boundary $\Gamma = \partial\Omega$ is subdivided in a finite number of arcs which can be represented through

$$x_1 = \chi_1(s), \quad x_2 = \chi_2(s), \quad s_m \leq s \leq s_M,$$

where the functions χ_α are assumed to be sufficiently smooth and such that $(\chi_1')^2 + (\chi_2')^2 \neq 0$ on $[s_m, s_M]$.

This domain Ω is approximated by a domain Ω_h as follows.

2.1. Exact triangulation of the domain Ω

This one is realized as in the case of a polygonal domain. The main difference is that the triangles K_c , with two vertices on the boundary, have two rectilinear sides and a curved third side located on the boundary.

2.2. The approximated domain Ω_h

We realize a P_5 -Hermite interpolation of the curved sides a_1a_2 of the triangles K_c so that these triangles K_c are replaced by triangles K (see Fig. 2.1) and then the domain Ω is replaced by a domain Ω_h .

More precisely, given the following parameterization of the arc a_1a_2 :

$$x_\alpha = \psi_\alpha(\hat{x}_2), \quad 0 \leq \hat{x}_2 \leq 1, \quad \text{with } \psi_\alpha(\hat{x}_2) = \chi_\alpha(\underline{s} + (\bar{s} - \underline{s})\hat{x}_2), \quad \alpha = 1, 2, \quad (2.1)$$

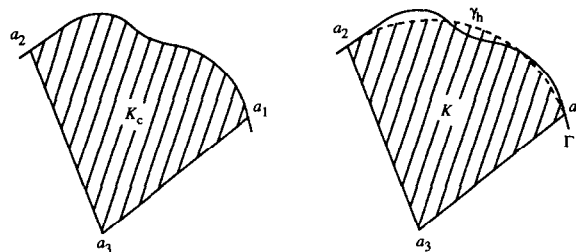


Fig. 2.1. The exact and approximated triangles K_c and K .

the arc γ_h is parameterized by

$$\psi_{h\alpha}(\hat{x}_2) = x_{\alpha 1} + (x_{\alpha 2} - x_{\alpha 1})\hat{x}_2 + \hat{x}_2(1 - \hat{x}_2) \left[\beta_{\alpha 3}(\hat{x}_2)^3 + \beta_{\alpha 2}(\hat{x}_2)^2 + \beta_{\alpha 1}\hat{x}_2 + \beta_{\alpha 0} \right], \quad (2.2)$$

where the coefficients $\beta_{\alpha l}$, $l = 0, 1, 2, 3$, are given by

$$\begin{cases} \beta_{\alpha 0} = x_{\alpha 1} - x_{\alpha 2} + (\bar{s} - \underline{s})\chi'_{\alpha}(\underline{s}), \\ \beta_{\alpha 1} = x_{\alpha 1} - x_{\alpha 2} + (\bar{s} - \underline{s})\chi'_{\alpha}(\underline{s}) + \frac{1}{2}(\bar{s} - \underline{s})^2\chi''_{\alpha}(\underline{s}), \\ \beta_{\alpha 2} = 9(x_{\alpha 2} - x_{\alpha 1}) - (\bar{s} - \underline{s})[5\chi'_{\alpha}(\underline{s}) + 4\chi'_{\alpha}(\bar{s})] - \frac{1}{2}(\bar{s} - \underline{s})^2[2\chi''_{\alpha}(\underline{s}) - \chi''_{\alpha}(\bar{s})], \\ \beta_{\alpha 3} = 6(x_{\alpha 1} - x_{\alpha 2}) + 3(\bar{s} - \underline{s})[\chi'_{\alpha}(\underline{s}) + \chi'_{\alpha}(\bar{s})] + \frac{1}{2}(\bar{s} - \underline{s})^2[\chi''_{\alpha}(\underline{s}) - \chi''_{\alpha}(\bar{s})]. \end{cases}$$

Let \hat{K} be the unit right-angled triangle. Then, we introduce the following extension $F_K : \hat{K} \rightarrow K$ of the application ψ_h :

$$\begin{aligned} F_{K_{\alpha}}(\hat{x}_1, \hat{x}_2) &= x_{\alpha 3} + (x_{\alpha 1} - x_{\alpha 3})\hat{x}_1 + (x_{\alpha 2} - x_{\alpha 3})\hat{x}_2 \\ &\quad + \frac{1}{2}\hat{x}_1\hat{x}_2 \left[\beta_{\alpha 3}(\hat{x}_2)^3 + \beta_{\alpha 2}(\hat{x}_2)^2 + \beta_{\alpha 1}\hat{x}_2 + \beta_{\alpha 0} + \tilde{\beta}_{\alpha 3}(\hat{x}_1)^3 + \tilde{\beta}_{\alpha 2}(\hat{x}_1)^2 + \tilde{\beta}_{\alpha 1}\hat{x}_1 + \tilde{\beta}_{\alpha 0} \right], \\ \alpha &= 1, 2, \end{aligned} \quad (2.3)$$

with

$$\begin{cases} \tilde{\beta}_{\alpha 0} = x_{\alpha 2} - x_{\alpha 1} - (\bar{s} - \underline{s})\chi'_{\alpha}(\bar{s}), \\ \tilde{\beta}_{\alpha 1} = x_{\alpha 2} - x_{\alpha 1} - (\bar{s} - \underline{s})\chi'_{\alpha}(\bar{s}) + \frac{1}{2}(\bar{s} - \underline{s})^2\chi''_{\alpha}(\bar{s}), \\ \tilde{\beta}_{\alpha 2} = 9(x_{\alpha 1} - x_{\alpha 2}) + (\bar{s} - \underline{s})[5\chi'_{\alpha}(\bar{s}) + 4\chi'_{\alpha}(\underline{s})] - \frac{1}{2}(\bar{s} - \underline{s})^2[2\chi''_{\alpha}(\bar{s}) - \chi''_{\alpha}(\underline{s})], \\ \tilde{\beta}_{\alpha 3} = 6(x_{\alpha 2} - x_{\alpha 1}) - 3(\bar{s} - \underline{s})[\chi'_{\alpha}(\bar{s}) + \chi'_{\alpha}(\underline{s})] + \frac{1}{2}(\bar{s} - \underline{s})^2[\chi''_{\alpha}(\bar{s}) - \chi''_{\alpha}(\underline{s})]. \end{cases}$$

In [3] we have proved the following theorem.

Theorem 2.1. For $h_K = \text{diam}(K)$ sufficiently small, we have

- (i) the application F_K is a \mathcal{C}^{∞} -diffeomorphism from \hat{K} onto \bar{K} ;
- (ii) the applications F_K and $F_K^{-1} : \bar{K} \rightarrow \hat{K}$ satisfy

$$\|F_K\|_{l, \infty, \hat{K}} = \sup_{\hat{x} \in \hat{K}} \|D^l F_K(\hat{x})\| \leq ch_K^l, \quad l = 0, 1, \dots, \quad (2.4)$$

$$\|F_K^{-1}\|_{l, \infty, K} = \sup_{x \in K} \|D^l F_K^{-1}(x)\| \leq ch_K^{-1}, \quad l = 1, 2, \dots; \quad (2.5)$$

- (iii) the Jacobians $J_{F_K}(\hat{x})$ and $J_{F_K^{-1}}(x)$ satisfy

$$c_1 h_K^2 \leq |J_{F_K}|_{0, \infty, \hat{K}} \leq c_2 h_K^2, \quad |J_{F_K}|_{l, \infty, \hat{K}} \leq ch_K^{2+l}, \quad l = 0, \dots, 5, \quad (2.6)$$

$$\frac{c_1}{h_K^2} \leq |J_{F_K^{-1}}|_{0, \infty, K} \leq \frac{c_2}{h_K^2}, \quad (2.7)$$

where c, c_1, c_2 denote constants > 0 , independent of h_K , which can change from one inequality to the next.

2.3. A curved finite element \mathcal{E}^1 -compatible with the Argyris triangle

The Argyris triangle [1] uses P_5 -polynomials and its set of degrees of freedom includes the values of the function and the values of the first and second partial derivatives at the vertices, and the values of the normal derivatives at midsides, i.e., 21 degrees of freedom.

The connection between a curved element and an Argyris triangle will be realized along the rectilinear sides a_3a_1 or a_3a_2 . In order to get a \mathcal{E}^1 -junction,

(i) it is necessary that

- along the sides a_3a_1 and a_3a_2 the degrees of freedom are the same as those of the Argyris triangle;
- the traces $p|_{[a_3a_\alpha]}$ (respectively $\partial p / \partial n_{3\alpha}|_{[a_3a_\alpha]}$), $\alpha = 1, 2$, of the shape functions p are polynomials of degree 5 (respectively 4), entirely determined by the degrees of freedom related to the sides a_3a_α , $\alpha = 1, 2$;

(ii) it is desirable for the approximation studies that the images $\hat{p} = p \circ F_K$ of the shape functions p are *polynomials*. In this way, we are led to use the basic finite element described on Fig. 2.2.

Indeed, $\hat{p} = p \circ F_K$ belongs to P_5 when restricted to the sides $\hat{a}_3\hat{a}_\alpha$. Likewise for any point $a \in [a_3a_2]$, we get

$$\frac{\partial \hat{p}}{\partial \hat{x}_1}(\hat{a}) = \left\langle \frac{\partial F_K}{\partial \hat{x}_1}(\hat{a}), \frac{a_2 - a_3}{|a_2 - a_3|^2} Dp(a)(a_2 - a_3) + \frac{a_1 - c_1}{|a_1 - c_1|^2} Dp(a)(a_1 - c_1) \right\rangle, \quad (2.8)$$

where c_1 is the orthogonal projection of a_1 on the side a_3a_2 . Then we check that $\partial \hat{p} / \partial \hat{x}_1|_{[\hat{a}_3\hat{a}_2]} \in P_8$, so that we have to use at least a basic finite element of degree 9.

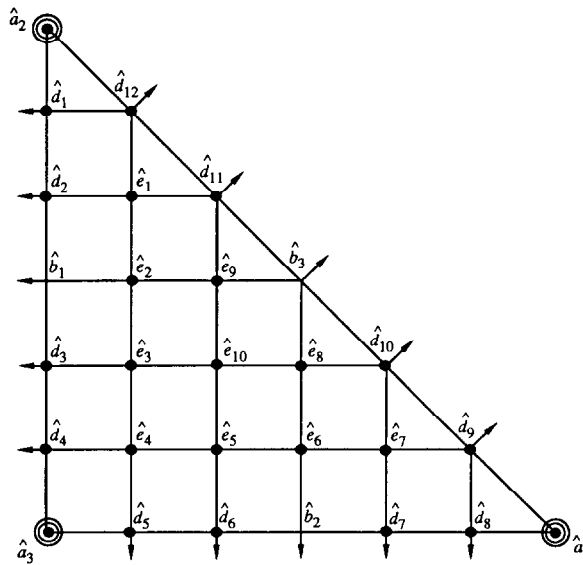


Fig. 2.2. Basic finite element for the construction of a curved finite element \mathcal{E}^1 -compatible with the Argyris triangle ($F_K \in (P_5)^2$). \hat{K} = unit right-angled triangle; $\hat{P} = P_9$; $\dim \hat{P} = 55$.

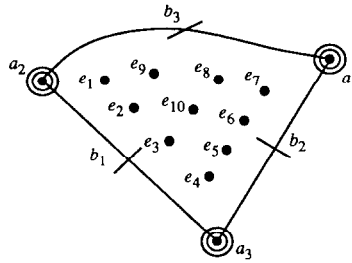


Fig. 2.3. The set of degrees of freedom Σ_K for the curved finite elements \mathcal{C}^1 -compatible with the Argyris finite element ($F_K \in (P_5)^2$).

Moreover, the degrees of freedom of the \mathcal{C}^1 -curved finite element are displayed on Fig. 2.3; they include the 21 degrees of freedom of the Argyris triangle plus ten internal degrees of freedom.

Given these prerequisites, let us describe how to construct the interpolating function $\pi_K v$ of a smooth v upon the curved triangle K (four points).

Point 1. For the given function v , compute the values of the 31 degrees of freedom Σ_K (see Fig. 2.3).

Point 2. From this set of values and by using the mapping F_K , we construct a suitable set of values of degrees of freedom for the basic finite element displayed on Fig. 2.2. More precisely,

- the values of the *eighteen degrees of freedom* located at the vertices are the images of the associated degrees of freedom of the curved element through the application F_K . The same holds true for the *ten internal degrees of freedom* located at point \hat{e}_i , $i = 1, \dots, 10$, and for the *normal derivative at point \hat{b}_3* ;

- along the sides $\hat{a}_3\hat{a}_1$, $\hat{a}_3\hat{a}_2$ and $\hat{a}_1\hat{a}_2$, we constrain the shape function to be a polynomial of degree 5 completely determined by the above values of the degrees of freedom at the vertices. Then, we get the *suitable twelve values* of the shape function at nodes \hat{d}_i , $i = 1, \dots, 12$;
- the knowledge of the shape function along the sides $\hat{a}_3\hat{a}_1$ and $\hat{a}_3\hat{a}_2$ gives the values of its derivative along these sides at points \hat{b}_1 and \hat{b}_2 . By adding the values of the images of the normal derivatives at points b_1 and b_2 through the mapping F_K (which are generally oblique derivatives at points \hat{b}_1 and \hat{b}_2), we obtain the suitable values of the normal derivative of the shape function at points \hat{b}_1 and \hat{b}_2 ;
- along the sides $\hat{a}_3\hat{a}_1$ and $\hat{a}_3\hat{a}_2$ we constrain the normal derivatives of the shape function to be a polynomial of degree 4 completely determined by the associated values of the normal derivative of the shape function at the vertices and at the midside. Then we get the twelve missing values of the normal derivatives at nodes \hat{d}_i , $i = 1, \dots, 12$.

Let us emphasize that this construction attributes a value at each degree of freedom of the basic finite element. These 55 values are only dependent on the 31 values of the degrees of freedom of the curved element, computed from the given function v .

Point 3. From this constrained set of 55 values of the degrees of freedom of the basic finite element (see Fig. 2.2), we obtain the corresponding P_9 -interpolation function, say \hat{w} , which is just depending on the 31 values of the degrees of freedom of function v .

Point 4. Then, we can check (see [3, Theorem 3.2]) that the function $\hat{w} \circ F_K^{-1}$ satisfies the interpolating properties so that the subsequent notation is justified:

$$\pi_K v = \hat{w} \circ F_K^{-1}. \quad (2.9)$$

2.4. Interpolation error estimate

In [3, Theorem 4.1], we have proved the following theorem.

Theorem 2.2. *There exists a constant C , independent of h_K , such that, for any curved finite element \mathcal{E}^1 -compatible with the Argyris triangle, we have*

$$|v - \pi_K v|_{m,K} \leq C h_K^{k+1-m} \|v\|_{k+1,K}, \quad \forall v \in H^{k+1}(K), \quad k = 3, \dots, 5, \quad 0 \leq m \leq k+1, \quad (2.10)$$

where $\pi_K v$ is the interpolating function given in (2.9).

2.5. Numerical tests of the interpolation properties

The implementation of this curved finite element is detailed in [6] where the reader can also find some numerical tests which prove the excellent interpolating properties. According to Theorem 2.2, we want to check that

$$|v - \pi_K v|_{m,K} \leq c h_K^{6-m} \|v\|_{6,K}, \quad \forall v \in H^6(K), \quad m = 0, \dots, 6. \quad (2.11)$$

Since the error norms $|\cdot|_{L^2(K)}$ and $|\cdot|_{L^\infty(K)}$ have the same order, we will just check that at a given point

$$\text{Log } |v - \pi_K v| = C + 6 \text{ Log } h_K. \quad (2.12)$$

In this way, consider the triangle K displayed on Fig. 2.4. Its curved side can be parameterized by

$$x_1 = \chi_1(s) = \cos s, \quad x_2 = \chi_2(s) = R \sin s, \quad 0 < R < 1, \quad \underline{s} = \frac{1}{6}\pi \leq s \leq \bar{s} = \frac{1}{3}\pi.$$

To check the relation (2.12), we introduce the sequence of nested triangles K_h displayed on Fig. 2.4 and we report on Fig. 2.5 the behaviour of $\text{Log } |v - \pi_K v|$ at point $F_{K_h}(\frac{3}{8}, \frac{3}{8})$ when $h_K \rightarrow 0$; the slope is exactly 6.

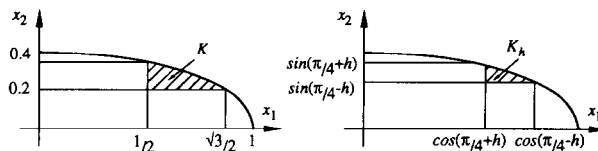


Fig. 2.4. The curved triangle K and the sequence of nested triangles K_h ($R = 0.4$).

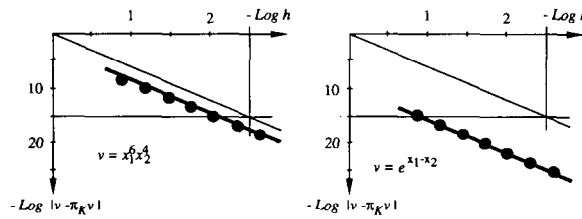


Fig. 2.5. Asymptotic behaviour of $|v - \pi_K v|$ at point $F_{K_h}(\frac{3}{8}, \frac{3}{8})$ when $h_K \rightarrow 0$.

3. Approximation of thin-plate and thin-shell problems

Since our thin-shell equations give back the thin-plate equations when the middle surface of the shell is plane, we consider the case of a thin-shell problem and we will just mention the modifications that we have to do in the particular case of a plate.

3.1. Variational formulation of a thin-shell problem

We will consider the general thin-shell equations given by Koiter [19]. For this modeling, the middle surface S of the shell is defined as the image of a plane reference domain Ω through a regular mapping ϕ . Then, the problem can be formulated as follows [2,5,11].

Problem 3.1. For $\phi \in (\mathcal{C}^3(\bar{\Omega}))^3$, for $\mathbf{p} \in (L^2(\Omega))^3$, find $\mathbf{u} \in V$ such that

$$a(\mathbf{u}, \mathbf{v}) = f(\mathbf{v}), \quad \forall \mathbf{v} \in V, \quad (3.1)$$

where the space V of the admissible displacements is given by

$$V = H_0^1(\Omega) \times H_0^1(\Omega) \times H_0^2(\Omega). \quad (3.2)$$

The bilinear form $a(\cdot, \cdot)$ and the linear form $f(\cdot)$ are given by

$$a(\mathbf{u}, \mathbf{v}) = \int_{\Omega} {}^t \mathbf{U} [A_{IJ}] \mathbf{V} \, d\xi^1 \, d\xi^2, \quad (3.3)$$

$$f(\mathbf{v}) = \int_{\Omega} {}^t \mathbf{F} \mathbf{V} \, d\xi^1 \, d\xi^2, \quad (3.4)$$

where

$${}^t \mathbf{V} = [v_1, v_{1,1}, v_{1,2}, v_2, v_{2,1}, v_{2,2}, v_3, v_{3,1}, v_{3,2}, v_{3,11}, v_{3,12}, v_{3,22}],$$

$${}^t \mathbf{F} = \sqrt{a} [p^1, 0, 0, p^2, 0, 0, p^3, 0, 0, 0, 0, 0],$$

and where the symmetrical matrix $[A_{IJ}]_{12 \times 12}$ takes into account the geometry of the shell and the mechanical characteristics of the material. Moreover, the data concern the case of a clamped shell which is loaded by a resultant of density \mathbf{p} on S . More general boundary conditions and more general loadings can be considered as well.

Theorem 3.2 (Bernadou, Ciarlet and Miara [8,9]). *Problem 3.1 has one and only one solution.*

For subsequent analysis, it is interesting to assume the following.

Hypothesis 3.3. *The mapping $\phi: \bar{\Omega} \subset \mathbb{R}^2 \rightarrow \bar{S} = \phi(\bar{\Omega})$ is defined on a domain $\tilde{\Omega} \supset \bar{\Omega}$, $\phi \in (\mathcal{C}^3(\tilde{\Omega}))^3$ and $\phi_{,1}(\xi) \times \phi_{,2}(\xi) \neq \mathbf{0}$ for any point $\xi = (\xi^1, \xi^2) \in \tilde{\Omega}$. Likewise, we assume that the loading $p \in (\mathcal{C}^0(\tilde{\Omega}))^3$.*

3.2. The discrete problem

By using the \mathcal{C}^1 -curved elements introduced in Section 2, we are going to extend to the general curved boundary reference domain Ω some previous results [2,5], valid for polygonal domains Ω . Such an extension is very interesting since

- (i) in many practical situations, the reference domains Ω have curved boundaries (domes, junctions of shells, ..., middle surfaces of plate problems, ...);
- (ii) it permits to develop a high-accuracy approximation method in these so common situations.

Domain Ω_h . According to Section 2.2, we consider the domain Ω_h which is such that

$$\bar{\Omega}_h = \bigcup_{K \in \mathcal{T}_h} \bar{K}, \quad \text{where } \mathcal{T}_h = \mathcal{T}_h^1 \cup \mathcal{T}_h^2.$$

Triangulation \mathcal{T}_h^1 collects the rectilinear triangles while \mathcal{T}_h^2 collects the curved triangles with one curved side interpolating an arc of the boundary.

Space V_h . Set $V_h = V_{h1} \times V_{h1} \times V_{h2}$. The space V_{h2} is constructed from the Argyris triangles for any $K \in \mathcal{T}_h^1$ and from the associated \mathcal{C}^1 -curved elements for any $K \in \mathcal{T}_h^2$; then we impose the clamped boundary conditions along $\partial\Omega_h$. Likewise, V_{h1} can be constructed from the same finite elements, or, by using the previous applications $F_K: \hat{K} \rightarrow K$, we can define \mathcal{C}^0 -finite elements for any $K \in \mathcal{T}_h^1$ and their associated \mathcal{C}^0 -curved elements for any $K \in \mathcal{T}_h^2$; in both cases, we impose simply supported boundary conditions along $\partial\Omega_h$. Then,

$$V_h \subset V(\Omega_h) = H_0^1(\Omega_h) \times H_0^1(\Omega_h) \times H_0^2(\Omega_h). \quad (3.5)$$

Hypothesis 3.3 involves the existence of $h_0 > 0$ such that

$$\Omega_h \subset \tilde{\Omega}, \quad \forall h \in]0, h_0[. \quad (3.6)$$

Numerical integration techniques

Upon the reference triangle \hat{K} we define the numerical integration scheme

$$\int_{\hat{K}} \hat{\phi}(\hat{x}) \, d\hat{x} \approx \sum_{l=1}^L \hat{\omega}_l \hat{\phi}(\hat{b}_l),$$

which induces the following numerical integration scheme upon the curved triangle $K = F_K(\hat{K})$:

$$\int_K \phi(x) \, dx \approx \sum_{l=1}^L \omega_{l,K} \phi(b_{l,K}),$$

where $\omega_{l,K} = \hat{\omega}_l J_{F_K}(\hat{b}_l)$, $b_{l,K} = F_K(\hat{b}_l)$, $l = 1, \dots, L$, and J_{F_K} = Jacobian of the mapping F_K (which is assumed > 0 without loss of generality).

The discrete problem

To the forms (3.3) and (3.4), we associate the approximated forms

$$\mathbf{u}_h, \mathbf{v}_h \in V_h \mapsto a_h(\mathbf{u}_h, \mathbf{v}_h) = \sum_{K \in \mathcal{T}_h} \sum_{l=1}^L \omega_{l,K} {}^t \mathbf{U}_h(b_{l,K}) [A_{IJ}(b_{l,K})] \mathbf{V}_h(b_{l,K}), \quad (3.7)$$

$$\mathbf{v}_h \in V_h \rightarrow f_h(\mathbf{v}_h) = \sum_{K \in \mathcal{T}_h} \sum_{l=1}^L \omega_{l,K} {}^t \mathbf{F}(b_{l,K}) \mathbf{V}_h(b_{l,K}). \quad (3.8)$$

Thanks to Hypotheses 3.3 and 3.4 the different terms of expressions (3.7), (3.8) make sense.

Hypothesis 3.4. Upon the reference triangle \hat{K} , all the integration nodes are internal or they coincide with the vertices \hat{a}_1 , \hat{a}_2 and \hat{a}_3 .

Then the *discrete problem* can be formulated as follows:

$$\text{Find } \mathbf{u}_h \in V_h \text{ such that } a_h(\mathbf{u}_h, \mathbf{v}_h) = f_h(\mathbf{v}_h), \quad \forall \mathbf{v}_h \in V_h. \quad (3.9)$$

As usual, the guidelines for the study of convergence and obtaining error estimates are contained in the following abstract error estimate.

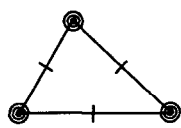
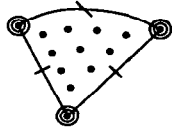
Argyris triangle ($K \in \mathcal{T}_h^1$)	C^1 -curved element ($K \in \mathcal{T}_h^2$)
	
<ul style="list-style-type: none"> • Error estimate in $O(h^4)$ • $A_{IJ} \in W^{4,\infty}(\hat{\Omega})$, $6 \leq I, J \leq 12$ • $\tilde{A} \tilde{u}_3 \in W^{4,q}(\hat{\Omega})$, $q \geq 2$; $\tilde{u}_3 \in H^6(\hat{\Omega})$ 	
<ul style="list-style-type: none"> • Scheme exact for P_6 • Suitable schemes with 12 nodes (see [15,17,22,23]) 	<ul style="list-style-type: none"> • Scheme exact for P_{14} • Suitable scheme with 42 nodes [17]

Fig. 3.1. Approximation of the bending of a thin plate whose middle plane has a curved boundary (error estimates, required regularity on data and solution and criteria on the numerical integration scheme).

Abstract error estimate

Theorem 3.5. Let (3.9) be a family of discrete problems satisfying hypotheses (3.5), (3.6) and such that there exists a constant $\beta > 0$, independent of h , such that

$$\beta \|v_h\|_{X(\Omega_h)}^2 \leq a_h(v_h, v_h), \quad \forall v_h \in V_h, \quad \forall h \text{ sufficiently small}, \quad (3.10)$$

where $X(\Omega_h) = (H^1(\Omega_h))^2 \times H^2(\Omega_h)$ and $\|v\|_{X(\Omega_h)} = [\|v_1\|_{1,\Omega_h}^2 + \|v_2\|_{1,\Omega_h}^2 + \|v_3\|_{2,\Omega_h}^2]^{1/2}$.

For any $v, w \in X(\Omega_h)$, the bilinear form $\tilde{a}_h(v, w)$ is defined by relation

$$\tilde{a}_h(v, w) = \int_{\Omega_h} {}^t \mathbf{V}[A_{IJ}] \mathbf{W} \, dx.$$

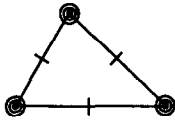
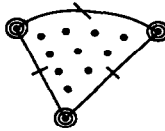
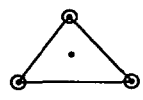

<div style="text-align: center;">Finite elements used to construct V_{h2}</div> <div style="text-align: center;">Finite elements used to construct V_{h1}</div>	<div style="text-align: center;">Argyris triangle ($K \in \mathcal{T}_h^1$)</div> 	<div style="text-align: center;">\mathcal{C}^1-curved element ($K \in \mathcal{T}_h^2$)</div> 
<div style="text-align: center;">Same elements than those used to construct V_{h2}</div>	<ul style="list-style-type: none"> • Error estimate in $O(h^4)$ • $A_{IJ} \in W^{4,\infty}(\tilde{\Omega})$; $\tilde{A}\tilde{u} \in (W^{4,q}(\tilde{\Omega}))^3$, $q \geq 2$ • $\tilde{u} \in (H^5(\tilde{\Omega}))^2 \times H^6(\tilde{\Omega})$ <div style="display: flex; justify-content: space-between;"> <div style="width: 45%;"> <ul style="list-style-type: none"> • Scheme exact for P_8 • Suitable schemes with 16 nodes [17,23] </div> <div style="width: 45%;"> <ul style="list-style-type: none"> • Schemes exact for P_{16} • Suitable schemes with (*) 52 nodes [17] but 3 are external to K so that Hypothesis 3.2 is not satisfied • (*) 61 nodes [17] </div> </div>	
<div style="text-align: center;">Hermite triangle of type 3 ($K \in \mathcal{T}_h^1$)</div>  <div style="text-align: center;">and \mathcal{C}^0-curved associated element ($K \in \mathcal{T}_h^2$)</div> 	<ul style="list-style-type: none"> • Error estimate in $O(h^3)$ • $A_{IJ} \in W^{3,\infty}(\tilde{\Omega})$; $\tilde{A}\tilde{u} \in (W^{3,q}(\tilde{\Omega}))^3$, $q \geq 2$ • $\tilde{u} \in (H^4(\tilde{\Omega}))^2 \times H^5(\tilde{\Omega})$ <div style="display: flex; justify-content: space-between;"> <div style="width: 45%;"> <ul style="list-style-type: none"> • Scheme exact for P_6 • Suitable schemes with 12 nodes [15,17,22,23] </div> <div style="width: 45%;"> <ul style="list-style-type: none"> • Schemes exact for P_{14} • Suitable schemes with 42 nodes [17] </div> </div>	

Fig. 3.2. Approximation of thin shells for a reference domain with curved boundary (error estimates, required regularity on data and solution and criteria on the numerical integration scheme).

Then, there exists a constant C , independent of h , such that

$$\begin{aligned} \|\tilde{\mathbf{u}} - \mathbf{u}_h\|_{X(\Omega_h)} \leq C \left[\inf_{\mathbf{v}_h \in V_h} \left\{ \|\tilde{\mathbf{u}} - \mathbf{v}_h\|_{X(\Omega_h)} + \sup_{\mathbf{w}_h \in V_h} \frac{|\tilde{a}_h(\mathbf{v}_h, \mathbf{w}_h) - a_h(\mathbf{v}_h, \mathbf{w}_h)|}{\|\mathbf{w}_h\|_{X(\Omega_h)}} \right\} \right. \\ \left. + \sup_{\mathbf{w}_h \in V_h} \frac{|\tilde{a}_h(\tilde{\mathbf{u}}, \mathbf{w}_h) - f_h(\mathbf{w}_h)|}{\|\mathbf{w}_h\|_{X(\Omega_h)}} \right], \end{aligned} \quad (3.11)$$

where $\tilde{\mathbf{u}}$ is any function of $V(\tilde{\Omega}) = (H_0^1(\tilde{\Omega}))^2 \times H_0^2(\tilde{\Omega})$.

In order to find an explicit estimate of the asymptotic error, we will take in (3.11) any extension $\tilde{\mathbf{u}}$ to the domain $\tilde{\Omega}$ of the solution \mathbf{u} , and we will have to

- (i) check the property (3.10);
- (ii) evaluate the error interpolation term in (3.11);
- (iii) evaluate the consistency terms in (3.11).

All these studies are detailed in [4] so that we just display the main results for plate and shell problems in Figs. 3.1 and 3.2.

References

- [1] J.H. Argyris, I. Fried and D.W. Scharpf, The TUBA family of plate elements for the matrix displacement method, *Aeronaut. J. Roy. Aeronaut. Soc.* **72** (1968) 701–709.
- [2] M. Bernadou, Convergence of conforming finite element methods for general shell problems, *Internat. J. Engrg. Sci.* **18** (1980) 249–276.
- [3] M. Bernadou, \mathcal{E}^1 -curved finite elements with numerical integration for thin plate and thin shell problems, Part 1: Construction and interpolation properties of curved \mathcal{E}^1 finite elements, *Comput. Methods Appl. Mech. Engrg.* **102** (2) (1993) 255–289.
- [4] M. Bernadou, \mathcal{E}^1 -curved finite elements with numerical integration for thin plate and thin shell problems, Part 2: Approximation of thin plate and thin shell problems, *Comput. Methods Appl. Mech. Engrg.* **102** (3) (1993) 389–421.
- [5] M. Bernadou and J.M. Boisserie, *The Finite Element Method in Thin Shell Theory: Application to Arch Dam Simulations* (Birkhäuser, Boston, MA, 1982).
- [6] M. Bernadou and J.-M. Boisserie, Curved finite elements of class C^1 : Implementation and numerical experiments. Part 1: Construction and numerical tests of the interpolation properties, *Comput. Methods Appl. Mech. Engrg.* **106** (1–2) (1993) 229–269.
- [7] M. Bernadou and J.M. Boisserie, Curved finite elements of class \mathcal{E}^1 : Implementation and numerical experiments. Part 2: Applications to thin plate and thin shell problems, *Rapports Rech. INRIA*, to appear.
- [8] M. Bernadou and P.G. Ciarlet, Sur l'ellipticité du modèle linéaire de coques de W.T. Koiter, in: R. Glowinski and J.L. Lions, Eds., *Computing Methods in Applied Sciences and Engineering*, Lectures Notes in Econom. and Math. Systems **134** (Springer, Berlin, 1976) 89–136.
- [9] M. Bernadou, P.G. Ciarlet and B. Miara, On the existence and uniqueness of a solution for some linear shell models, *J. Elasticity*, to appear.
- [10] M.W. Chernuka, G.R. Cowper, G.M. Lindberg and M.D. Olson, Finite element analysis of plates with curved edges, *Internat. J. Numer. Methods Engrg.* **4** (1972) 49–65.
- [11] P.G. Ciarlet, Conforming finite element methods for thin shell problems, in: J.R. Whiteman, Ed., *Mathematics of Finite Elements and Applications II* (Academic Press, London, 1976) 105–123.
- [12] P.G. Ciarlet, *The Finite Element Method for Elliptic Problems*, Stud. Math. Appl. **4** (North-Holland, Amsterdam, 1978).

- [13] P.G. Ciarlet, Basic error estimates for elliptic problems, in: P.G. Ciarlet and J.L. Lions, Eds., *Handbook of Numerical Analysis, Vol. II: Finite Element Methods, Part 1* (North-Holland, Amsterdam, 1991) 17–351.
- [14] P.G. Ciarlet and P.-A. Raviart, Interpolation theory over curved elements, with applications to finite element methods, *Comput. Methods Appl. Mech. Engrg.* **1** (2) (1972) 217–249.
- [15] G.R. Cowper, Gaussian quadrature formulas for triangles, *Internat. J. Numer. Methods Engrg.* **7** (3) (1973) 405–408.
- [16] J. Douglas, T. Dupont, P. Percell and R. Scott, A family of \mathcal{C}^1 -finite elements with optimal approximation properties for various Galerkin methods for 2nd and 4th order problems, *RAIRO Anal. Numér.* **13** (1979) 227–256.
- [17] D.A. Dunavant, High degree efficient symmetrical Gaussian quadrature rules for the triangle, *Internat. J. Numer. Methods Engrg.* **21** (1985) 1129–1148.
- [18] T.M. Hruđey, A finite element procedure for plates with curved boundaries, *Comput. & Structures* **7** (1977) 553–564.
- [19] W.T. Koiter, On the foundations of the linear theory of thin elastic shells, *Proc. Kon. Nederl. Akad. Wetensch.* **B73** (1970) 169–195.
- [20] V.G. Korneev and S.E. Ponomarev, Use of curvilinear finite elements in schemes for solving linear elliptic equations of order $2n$, Part I, *Chisl. Metody Mekh. Sploshn. Sredy Novosibirsk* **5** (5) (1974) 78–97 (in Russian; English translation: UCRL trans. 10852).
- [21] V.G. Korneev and S.E. Ponomarev, Use of curvilinear finite elements in schemes for solving linear elliptic equations of order $2n$, Part II, *Chisl. Metody Mekh. Sploshn. Sredy Novosibirsk* **6** (1) (1975) 47–64 (in Russian).
- [22] M.E. Laursen and M. Gellert, Some criteria for numerically integrated matrices and quadrature formulas for triangles, *Internat. J. Numer. Methods Engrg.* **12** (1978) 67–76.
- [23] J.N. Lyness and D. Jespersen, Moderate degree symmetric quadrature rules for the triangles, *J. Inst. Math. Appl.* **15** (1975) 19–32.
- [24] L.E. Mansfield, Approximation of the boundary in the finite element solution of fourth order problems, *SIAM J. Numer. Anal.* **15** (1978) 568–579.
- [25] L.E. Mansfield, A Clough–Tocher type element useful for fourth order problems over non-polygonal domains, *Math. Comp.* **32** (1978) 135–142.
- [26] R. Scott, Interpolated boundary conditions in the finite element method, *SIAM J. Numer. Anal.* **12** (3) (1975) 404–427.
- [27] R. Scott, A survey of displacement methods for the plate bending problem, in: K.-J. Bathe, J.T. Oden and W. Wunderlich, Eds., *Proc. US–Germany Symp. on Formulations and Computational Algorithms in Finite Element Analysis* (MIT Press, Cambridge, MA, 1976) 855–876.
- [28] A. Ženišek, Curved triangles finite $\mathcal{C}^{(m)}$ -elements, *Apl. Mat.* **23** (1978) 346–377.
- [29] M. Zlámal, The finite element method in domains with curved boundaries, *Internat. J. Numer. Methods Engrg.* **5** (1973) 367–373.
- [30] M. Zlámal, Curved elements in the finite element method, Part I, *SIAM J. Numer. Anal.* **10** (1973) 229–240.
- [31] M. Zlámal, Curved elements in the finite element method, Part II, *SIAM J. Numer. Anal.* **11** (1974) 347–362.